Bilinear Modelling, Control and Stability of Directional Drilling

Isonguyo J. Inyang[a,*], James F. Whidborne[b]

[a]*Advanced Vehicle Engineering Centre, Cranfield University, UK*
[b]*Centre for Aeronautics, Cranfield University, UK*

Abstract

This paper proposes an approach for the attitude control of directional drilling tools for the oil and gas industry. A bilinear model of the directional drilling tool is proposed and it characterises the nonlinear properties of the directional drilling tool more accurately than the existing linear model, hence broadens the range of adequate performance. The proposed bilinear model is used as the basis for the design of a Bilinear Proportional plus Integral (BPI) controller. The stability of the proposed BPI control system is proven using stability notions for LTI and LPV systems. The transient simulation results show that the proposed BPI controller is more effective, robust and stable for the attitude control of the directional drilling tool than the existing PI controller. The proposed BPI controller provides improved invariant azimuth responses and significantly reduces the adverse effects of measurement delays and disturbances with respect to stability and performance of the directional drilling tool.

Keywords: Directional drilling, Attitude control, Bilinear, Time delay, Disturbances, Linear Parameter-Varying (LPV) systems

1. Introduction

In the oil and gas industry, directional drilling is the practice of creating a geometric wellbore with a directional drilling tool along a predetermined target

---

*Corresponding author
Email addresses: `i.inyang@cranfield.ac.uk` or `isonginyang@yahoo.com` (Isonguyo J. Inyang), `j.f.whidborne@cranfield.ac.uk` (James F. Whidborne)

underneath the Earth's surface for the extraction of petroleum hydrocarbons.
The application of directional drilling creates access to challenging petroleum reservoirs by allowing for the drilling of wells with complex geometries and longer reaching wells (Pedersen et al., 2009). Directional drilling involves attitude, that is, inclination and azimuth angles control of the directional drilling tool. The automatic control of the attitude of the directional drilling tool plays an important role in the maximisation of production as well as reduction of cost per foot of borehole. With the finite reserves of oil and gas resources, reduction in the cost per barrel is desired to cost-effectively match the growing energy requirements for the immediate future.
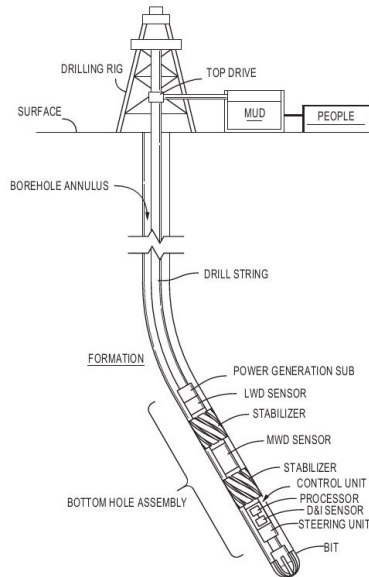

Figure 1: Main components of directional drilling system (Panchal, 2013)

A typical directional drilling system with its main components is shown in Fig. 1. During the directional drilling, the drill string, which is the combination of the Bottom-Hole Assembly (BHA) and drill pipe, provides the transmission of torque (from the top drive, located at the surface) and weight to the bit (located downhole). The bit crushes the rock during the propagation of the wellbore. The drilling mud is circulated from the surface to the bit via the drill string to

2

₂₀ lubricate and cool the rock cushing operation and to move the rock-cuttings to the surface via the annulus, that is, the gap between the wellbore and the drill pipe. At the surface, the removal of the cuttings is done, and the recirculation of the drilling fluid is carried out. The BHA comprises of Measurement While Drilling (MWD) subsystem, Logging While Drilling (LWD) subsystem, Power ₂₅ Generation Module (PGM), control unit, Direction and Inclination (D&I) sensor, steering unit and stabilisers. The LWD subsystem handles the surveys, measurements and assessments of formation properties while a wellbore is propagated, and sometimes shortly after the wellbore propagation, that is, during the periodical stop of the directional drilling operation. The MWD subsystem han- ₃₀ dles the surveys, measurements and assessments of physical parameters while a wellbore is propagated. The steering assembly (unit) allows for the direction and curvature of the directional drilling tool to be changed as desired during the propagation of the wellbore. Further details of directional drilling system and its operations can be found in Short (1993); Devereux (1999); Baker (1996) ₃₅ and Inyang (2017).

The control unit implements the control algorithms to provide attitude and trajectory control during the directional drilling operations. Note that there is limited communication between the surface and downhole. For example, mud pulse telemetry (Downton, 2012, 2014), which is a technique for the transmis- ₄₀ sion of commands from the surface to downhole and vice versa, provides about 1 bit/sec and about 100 bits/sec communication rates in the less and most favourable of conditions, respectively (Downton, 2012). This technique is significantly affected by measurement noise, the temporal and spatial sampling frequency, and the variability and magnitude of the telemetry delays (Jijón ₄₅ et al., 2010). Hence, the control algorithms must be implemented in the directional drilling tool downhole. The borehole can be several kilometres deep, and the environment is very harsh. The limited power supply and the harsh environment necessitate that the control algorithms must be simple.

To measure the attitude of the directional drilling tool, the D&I sensor is ₅₀ used, which senses the azimuth angle, θ_{azi} and inclination angle, θ_{inc} shown in

3

Fig. 2. The azimuth angle, $\theta_{\text{azi}} \in [0°, 360°)$ is evaluated relative to the Earth's magnetic field projection in the horizontal plane, where $0°$, $90°$, $180°$ and $270°$ correspond to due North, East, South and West, respectively. The inclination angle, $\theta_{\text{inc}} \in [0°, 180°]$ is the angular deviation from the vertical with $0°$, $90°$ and $180°$ defined downward, horizontal and upward, respectively.
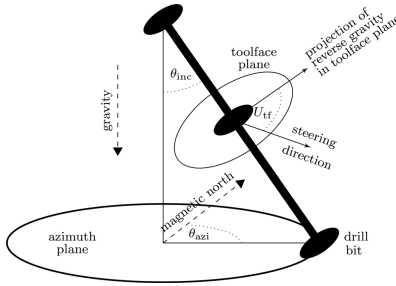

Figure 2: Typical steering and attitude parameters of directional drilling tool

This paper presents the design of a generic tool-independent attitude control algorithm for application to directional drilling tools. The significance of attitude control of directional drilling tools is highlighted in Genevois et al. (2003) and Yonezawa et al. (2002), where control techniques are proposed for the orientation of the borehole propagation based on holding the toolface angle. Genevois et al. (2003) described the desire for closed-loop "shoot and forget systems" and illustrated the azimuth control to be the major challenge. Most of the attitude control techniques described in literature are elucidated based on specific tool structures. Typical examples are by Yinghui and Yinao (2000), Genevois et al. (2003) and Yonezawa et al. (2002). Another interesting example presented by Kuwana et al. (1994) is an attitude controlling system which uses two-way telemetry communication links with the surface. The steering correction, calculated from the telemetry, is determined and then manually downlinked to the tool. Other control strategies recently developed include a hybrid approach consisting of two levels of automation for trajectory control of the tool (Matheus et al., 2014, 2012), a dynamic state-feedback controller design for 3D directional drilling systems (van de Wouw et al., 2016), a model-based robust

4

controller (Kremers et al., 2016), a robust Proportional plus Integral (PI) feedback controller (Panchal et al., 2010), an optimal H_∞ controller (Bayliss and Whidborne, 2015) and a linear quadratic Gaussian controller (Bayliss et al., 2015).

When modelling physical systems, the dynamics are often approximated as being linear models obtained by a first-order Taylor series approximation of the nonlinear model at a particular point of operation. It is clear that such linear models might be inaccurate over a wider range of operation; hence, bilinear models have been proposed to more accurately describe the nonlinear systems (see Bruni et al. (1974); Schwarz and Dorissen (1989)). Bilinear models can characterise nonlinear properties over a wider range of operations, hence, broaden the range of adequate performances and they are considered to be significantly advantageous in applications to practical industrial systems (Martineau et al., 2002). In this paper, a bilinear model of the directional drilling tool is developed by applying the Carleman bilinearisation technique (Ghasemi et al., 2014; Krener, 1974; Rugh, 1981). The generalised state space representation of a Multiple-Input Multiple-Output (MIMO) continuous-time bilinear system is expressed as (Kim and Lim, 2003):

$$\dot{x} = Ax + \left(B + \sum_{i=1}^{N} x_i M_i \right) u \tag{1}$$

where A, B and M_i are constant matrices of suitable dimensions, $u \in \mathbb{R}^{m \times 1}$ denotes the control vector, $x \in \mathbb{R}^{n \times 1}$ represents the vector of state variables and N denotes the number of expansion terms and augmented states.

The PI controller proposed by Panchal et al. (2010) provides good performance for the attitude control of the directional drilling tool but is insufficiently robust to cope with the disturbances and long time delay on the feedback measurements. Furthermore, it is designed at a particular operating point, hence leading to the inconsistency of the azimuth responses for different operating points. These disturbances are as a result of varying rock formations, a proclivity for the tool to drift horizontally, and to drop towards a vertical orientation due to gravity. While the long time delay arises because the D&I sensor which

5

measures the attitude change is, by necessity, located some distance (sometimes several tens of feet) behind the bit. The time delay increases with the distance of the D&I sensor from the bit, and inversely proportional to the Rate of Penetration (ROP).

To handle these disturbances, measurement delay and inconsistency of the azimuth responses in the attitude control of the directional drilling tool, this paper, with the extension of some of the works of Panchal et al. (2010) and Inyang et al. (2016), presents the design of a Bilinear Proportional plus Integral (BPI) controller which automatically holds the attitude of directional drilling tools at the desired attitude, and also significantly reduce the adverse effects of disturbances and measurement delay on stability and performance of directional drilling tools. The BPI controller is considered to provide more consistent azimuth responses over a wider range of directional drilling tool operations. The BPI controller, similar to the Bilinear Proportional-Integral-Derivative (BPID) controllers presented in Martineau et al. (2002, 2004) and Burnham et al. (1999) used in industrial furnace, is relatively simple compared to some of the existing bilinear controllers presented in Lim et al. (2009), Park and Lee (2009), Kim and Lim (2003), Goodhart et al. (1994), Chen et al. (2000), Qian and Zhang (2014), Kelman and Borrelli (2011) and Al-zahrani and Wali (1994) that are used in other different applications. Hence, given the relative simplicity of the BPI controller, it can easily be implemented in directional drilling tools to increase the potential of accessing difficult reservoirs, drilling more effectively and cost-effective field development.

The main contributions of this paper include: (1) The development of a bilinear model of the directional drilling tool which characterises the nonlinear properties of the directional drilling tool more accurately than the existing linear model, hence broadens the range of adequate performance. The proposed bilinear model of the directional tool is used for the design of the BPI controller. (2) The design of a BPI controller for the attitude control of the directional drilling tool. The proposed BPI controller is able to hold the attitude of the directional drilling tool at the desired inclination and azimuth angles and pro-

6

vide more consistent azimuth responses over wider range of directional drilling
operations. Furthermore, it significantly reduces the adverse effects of time delay on the feedback measurements, disturbances and some other uncertainties (such as drilling cycle and toolface actuator dynamics) in the attitude control of the directional drilling tool.

The remainder of this paper is organised as follows: Section 2 summarises some of the previous models of the directional drilling tool that are related to this paper; and also presents the development and the accuracy of a bilinear model of the directional drilling tool. Section 3 presents the design of a BPI controller for the attitude control of the directional drilling tool. In Section 4, the stability of the proposed BPI control system is proven using stability notions for Linear Time Invariant (LTI) and Linear Parameter-Varying (LPV) systems. Section 5 presents transient results based on Low-Fidelity Model (LFM) and High-Fidelity Model (HFM) simulations.

2. Models of Directional Drilling Tool

2.1. Previous Models

The directional drilling tool model proposed by Panchal et al. (2010) is derived from kinematic considerations and does not take into consideration the torsional and lateral dynamics of the drillstem and BHA. The model proposed by Panchal et al. (2010) is illustrated in Fig. 2 and it is given as:

$$\dot{\theta}_{\text{inc}} = V_{\text{rop}} \left(U_{\text{dls}} \cos U_{\text{tf}} - V_{\text{dr}} \right) \tag{2}$$

$$\dot{\theta}_{\text{azi}} = \frac{V_{\text{rop}}}{\sin \theta_{\text{inc}}} \left(U_{\text{dls}} \sin U_{\text{tf}} - V_{\text{tr}} \right) \tag{3}$$

where V_{rop} denotes the rate of penetration, a time-varying parameter, V_{tr} denotes the turn rate bias disturbance, V_{dr} denotes the drop rate disturbance ($V_{\text{dr}} = \alpha \sin \theta_{\text{inc}}$), α is a constant, U_{dls} denotes the curvature, also known as "dogleg severity" which is the product of duty cycle and K_{dls}, K_{dls} denotes the open-loop curvature capability of the tool, U_{tf} denotes the toolface angle control input, θ_{azi} denotes the azimuth angle and θ_{inc} denotes the inclination

angle. Note that in (3) there is a singularity when $\theta_{\text{inc}} = 0°$, hence, the model, (2) and (3) is restricted to attitudes such that θ_{inc} is not close to $0°$.

The model, (2) and (3) has also been used in Matheus et al. (2014, 2012) (see also Cockburn et al. (2011); Matheus and Naganathan (2010)) where field tested results are presented that show the fidelity of the model with actual practice.

The model, (2) and (3) is partially linearised and decoupled as follows (Panchal et al., 2010):

$$\dot{\theta}_{\text{inc}} = V_{\text{rop}} K_{\text{dls}} U_{\text{inc}} \tag{4}$$

$$\dot{\theta}_{\text{azi}} = \frac{V_{\text{rop}}}{\sin \theta_{\text{inc}}} K_{\text{dls}} U_{\text{azi}} \tag{5}$$

where U_{inc} and U_{azi} represent the virtual controls for the inclination and azimuth, respectively, and the transformation is given as: $U_{\text{tf}} = \text{ATAN2}\,(U_{\text{azi}}, U_{\text{inc}})$ and $U_{\text{dls}} = K_{\text{dls}}\sqrt{(U_{\text{azi}})^2 + (U_{\text{inc}})^2}$. With the linearisation of (4) and (5) about a nominal inclination angle, $\hat{\theta}_{\text{inc}}$, a linearised model of the directional drilling tool is obtained as follows (Panchal et al., 2010):

$$\dot{x}_{\text{inc}} = a u_{\text{inc}} \tag{6}$$

$$\dot{x}_{\text{azi}} = c x_{\text{inc}} + b u_{\text{azi}} \tag{7}$$

where $c = -b \cot \hat{\theta}_{\text{inc}}$, $b = a \csc \hat{\theta}_{\text{inc}}$ and $a = V_{\text{rop}} K_{\text{dls}}$. Based on (6) and (7), Panchal et al. (2010) designed a PI controller for the attitude control of the directional drilling tool.

2.2. Proposed Bilinear Model

In this subsection, the Carleman bilinearisation technique (Ghasemi et al., 2014; Krener, 1974; Rugh, 1981) is applied to the partially linearised and decoupled system, (4) and (5), to obtain a bilinear model of the directional drilling tool. Equations (4) and (5) are rewritten as:

$$\dot{\theta}_{\text{inc}} = a U_{\text{inc}} \tag{8}$$

$$\dot{\theta}_{\text{azi}} = \frac{a}{\sin \theta_{\text{inc}}} U_{\text{azi}} \tag{9}$$

8

where $a = V_{\mathrm{rop}} K_{\mathrm{dls}}$. Defining an augmented state vector for the Carleman bilinearisation as:

$$x^{\otimes} = [x_1, x_1^{(2)}, x_1^{(3)}, x_1^{(4)}, ..., x_1^{(N)}, x_2]^T \tag{10}$$

where $x_1 = \theta_{\mathrm{inc}}$, $x_2 = \theta_{\mathrm{azi}}$ and $\dot{x}_1^{(i)} = \frac{d}{dt}\left[(x_1)^i\right] = i\dot{x}_1 x_1^{(i-1)}$ leads to an extended bilinear state space system:

$$\dot{x}_1 = aU_{\mathrm{inc}} \tag{11}$$

$$\dot{x}_2 = aU_{\mathrm{azi}} \csc(x_1) = aU_{\mathrm{azi}} \sec(\beta) = aU_{\mathrm{azi}} \sum_{i=1}^{\infty} b_i x_1^{(i)} \tag{12}$$

where $\beta = \pi/2 - \theta_{\mathrm{inc}}$ and b_i are the coefficients of the Taylor series expansion of $\sec(\beta)$. The expansion of $\sec(\beta)$ is used instead of $\csc(x_1)$ so that the required powers of $x_1^{(i)}$ can be obtained from the θ_{inc} state equation. The Taylor series expansion of $\sec(\beta)$ for $-\frac{\pi}{2} < \beta < \frac{\pi}{2}$ is obtained from

$$\sec(\beta) = 1 + \frac{1}{2}\beta^2 + \frac{5}{24}\beta^4 + \frac{61}{720}\beta^6 + \cdots + \frac{(-1)^n E_{2n}(\beta)^{2n}}{(2n)!} + \ldots \tag{13}$$

150   where E_{2n} is the Euler number (Rade and Westergren, 1999, pp 81-99).

In practice, the number of terms in the series expansion and the number of augmented states is truncated to a finite value N (where N is equal to the number of expansion terms and augmented states) to an arbitrary degree of accuracy. Expanding (12), then (11) and (12) gives the bilinear system:

$$\dot{x}_1 = aU_{\mathrm{inc}} \tag{14}$$

$$\dot{x}_1^{(2)} = 2x_1\dot{x}_1 = 2ax_1 U_{\mathrm{inc}}$$

$$\dot{x}_1^{(3)} = 3x_1^{(2)}\dot{x}_1 = 3ax_1^{(2)} U_{\mathrm{inc}}$$

$$\vdots \qquad \vdots$$

$$\dot{x}_1^{(N)} = Nx_1^{(N-1)}\dot{x}_1 = Nax_1^{(N-1)} U_{\mathrm{inc}}$$

$$\dot{x}_2 = aU_{\mathrm{azi}} \sum_{i=1}^{N} b_i x_1^{(i)}$$

which is in the form of (1); where $A = [\ ]$, $u = [U_{\mathrm{inc}}, U_{\mathrm{azi}}]^T$ and $x = x^{\otimes}$. For

9

example, where $N = 3$, the following is obtained:

$$\begin{bmatrix} x_1 \\ x_1^{(2)} \\ x_1^{(3)} \\ x_2 \end{bmatrix} = \begin{bmatrix} 0 & 0 \\ 2a & 0 \\ 0 & 0 \\ 0 & ab_1 \end{bmatrix} \begin{bmatrix} U_{\text{inc}} \\ U_{\text{azi}} \end{bmatrix} x_1 + \begin{bmatrix} 0 & 0 \\ 0 & 0 \\ 3a & 0 \\ 0 & ab_2 \end{bmatrix} \begin{bmatrix} U_{\text{inc}} \\ U_{\text{azi}} \end{bmatrix} x_1^{(2)} \qquad (15)$$

$$+ \begin{bmatrix} 0 & 0 \\ 0 & 0 \\ 0 & 0 \\ 0 & ab_3 \end{bmatrix} \begin{bmatrix} U_{\text{inc}} \\ U_{\text{azi}} \end{bmatrix} x_1^{(3)} + \begin{bmatrix} a & 0 \\ 0 & 0 \\ 0 & 0 \\ 0 & 0 \end{bmatrix} \begin{bmatrix} U_{\text{inc}} \\ U_{\text{azi}} \end{bmatrix}$$

The accuracy of the proposed bilinear model of the directional drilling tool is analysed in the remaining part of this section. Furthermore, the proposed bilinear model is used as the basis for the BPI controller design as analysed in Section 3.

2.2.1. Bilinear Model Accuracy

To demonstrate the accuracy of the proposed bilinear model of the directional drilling tool, the transient azimuth responses for the open-loop systems using the proposed bilinear model for $N = 3$, 4 and 10 are analysed and compared with those from the nonlinear model, (2) and (3) (with V_{dr} and V_{tr} ignored) and the linear model, (6) and (7) proposed by Panchal et al. (2010). It is expected that the inclination responses of the models are identical because there is no nonlinearity in the inclination open-loops of the models. The parameters used for the models comparison simulation are given in Table 1.

Table 1: Simulation Parameters for Models Comparison

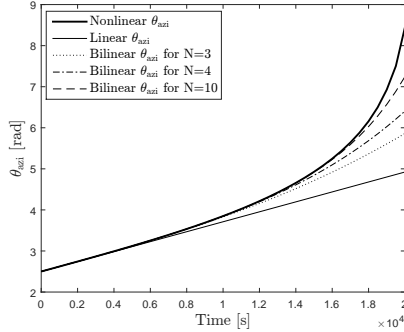| Parameter	Value	Parameter	Value
θ_{azi}	2.5 rad (143.24°)	V_{rop}	100 ft/hr (0.5079 m/min)
N	3, 4, 10	K_{dls}	10°/100 ft (5.7264e-3 rad/m)

10

Figure 3: Comparison of azimuth responses of nonlinear, linear and bilinear for $N = 3$, 4 and 10 models
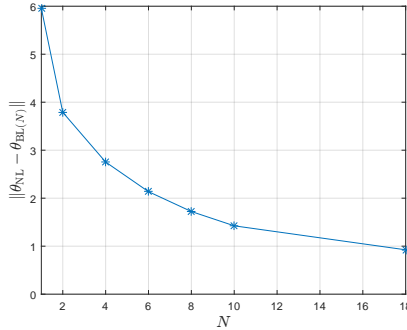

Figure 4: Relationship between the accuracy of bilinear azimuth responses and N

Based on the comparison shown in Fig. 3, the azimuth responses of the proposed bilinear model for $N = 3$, 4 and 10, where the accuracy of the proposed bilinear model improves as N increases, converge more closely to the azimuth response of the nonlinear model than that of the linear model. Hence, the proposed bilinear model characterises the nonlinear model more accurately than the linear model proposed by Panchal et al. (2010), thereby broadening the range of adequate performances, and it is considered to be significantly advantageous in applications to directional drilling operations.

Furthermore, to demonstrate that the accuracy of the proposed bilinear model increases with N, the norm error of the nonlinear and bilinear azimuth responses given by $\|\theta_{\mathrm{NL}} - \theta_{\mathrm{BL}(N)}\|$ as a function of N is shown in Fig. 4,

11

where θ_{NL} is the nonlinear azimuth response and $\theta_{\mathrm{BL}(N)}$ is the bilinear azimuth responses for $N = 1, 2, 4, 6, 8, 10$ and 18. Based on Fig. 4, it is analysed that $\|\theta_{\mathrm{NL}} - \theta_{\mathrm{BL}(N)}\|$ decreases as N increases. Hence, the accuracy of the proposed bilinear model improves as N increases.

3. BPI Controller Design

The proposed BPI controller design scheme, shown in Fig. 5, is based on the works of Martineau et al. (2002, 2004) and Burnham et al. (1999), and it is a combination of a bilinear compensator and a standard linear PI controller. The proposed bilinear compensator is only incorporated in the azimuth feedback loop to account for the nonlinear $1/\sin\theta_{\mathrm{inc}}$ term in (3).
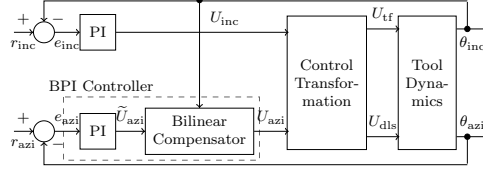

Figure 5: BPI control scheme

3.1. PI Controller

The PI control for the inclination and azimuth control channels are as follows, respectively:

$$U_{\mathrm{inc}} = k_{\mathrm{pi}}e_{\mathrm{inc}} + k_{\mathrm{ii}} \int_0^t e_{\mathrm{inc}}dt \tag{16}$$

$$\widetilde{U}_{\mathrm{azi}} = k_{\mathrm{pa}}e_{\mathrm{azi}} + k_{\mathrm{ia}} \int_0^t e_{\mathrm{azi}}dt \tag{17}$$

where $\widetilde{U}_{\mathrm{azi}}$ is the control input to the proposed bilinear compensator; $e_{\mathrm{inc}} = r_{\mathrm{inc}} - \theta_{\mathrm{inc}}$ and $e_{\mathrm{azi}} = r_{\mathrm{azi}} - \theta_{\mathrm{azi}}$; r_{inc} and r_{azi} are the nominal operating points for inclination and azimuth, respectively; k_{pi} and k_{ii} are the proportional and integral gains in the inclination feedback loop, respectively; k_{pa} and k_{ia} are
the proportional and integral gains in the azimuth feedback loop, respectively.

12

The gains for the PI controllers in the inclination and azimuth feedback loops are manually tuned to achieve desired performance in terms of zero steady state error, fast settling time and minimal overshoot, with practical engineering considerations.

3.2. Bilinear Compensator

Assuming that in Fig. 5, $U_{\mathrm{azi}} = \widetilde{U}_{\mathrm{azi}}$, then only the PI controller is incorporated (see (17)), and the azimuth feedback loop is expressed based on (12) as follows:

$$\dot{\theta}_{\mathrm{azi}} = a \sum_{i=1}^{\infty} b_i x_1^{(i)} (k_{\mathrm{pa}} e_{\mathrm{azi}} + k_{\mathrm{ia}} \int_0^t e_{\mathrm{azi}} dt) \tag{18}$$

Based on (13) and (14), (18) can further be expressed as:

$$\dot{\theta}_{\mathrm{azi}} = a(1 + \frac{1}{2}\beta^2 + \frac{5}{24}\beta^4 + \frac{61}{720}\beta^6 + \cdots + \frac{(-1)^n E_{2n}(\beta)^{2n}}{(2n)!}$$
$$+ \ldots)(k_{\mathrm{pa}} e_{\mathrm{azi}} + k_{\mathrm{ia}} \int_0^t e_{\mathrm{azi}} dt) \tag{19}$$

To account for the nonlinearity in (19), a bilinear compensator is proposed for the azimuth feedback loop which is given as:

$$\frac{U_{\mathrm{azi}}}{\widetilde{U}_{\mathrm{azi}}} = \frac{1}{1 + \frac{1}{2}\beta^2 + \frac{5}{24}\beta^4 + \frac{61}{720}\beta^6 + \cdots + \frac{(-1)^n E_{2n}(\beta)^{2n}}{(2n)!} + \ldots} \tag{20}$$

Clearly, this has an infinite number of terms, hence, for practical implementation, (20) is truncated at β^4, and it is given as:

$$\frac{U_{\mathrm{azi}}}{\widetilde{U}_{\mathrm{azi}}} = \frac{1}{1 + \frac{1}{2}\beta^2 + \frac{5}{24}\beta^4} \tag{21}$$

Note that, the simulation results of (20) truncated at degrees higher than β^4, have no significant improvement compared to those of (21).

The proposed bilinear compensator, (21) approximately cancels out the nonlinear $1/\sin\theta_{\mathrm{inc}}$ term in (3), thereby enhancing the performance of the PI con-
troller. The proposed bilinear compensator, (21), in combination with the PI controller, facilitates the ensuing BPI controller to sustain a required degree of control throughout a broader scope of operation about the tuning point compared with that obtained with the PI controller proposed by Panchal et al.

13

(2010). Hence, the proposed BPI controller design provides improved invariant

azimuth responses, and also reduces the adverse effects of measurement delays and disturbances with respect to stability and performance when compared with those obtained with the PI controller proposed by Panchal et al. (2010), as analysed in Section 5. However, as earlier mentioned in Section 2.1, there is a singularity in (3) when $\theta_{\text{inc}} = 0°$, hence, the proposed BPI controller is restricted to attitudes such that θ_{inc} is not close to $0°$.

The proposed BPI controller is relatively simple and it can easily be implemented in the directional drilling tools to increase the potential of accessing difficult reservoirs, drilling more effectively and cost-effective field development.

4. Stability Analysis of BPI Control System

The proposed BPI control system is shown in Fig. 6. From Fig. 6, it is clear that the stability of the proposed BPI control system can be analysed by considering the stability of the two feedback loops (inclination and azimuth) separately. With reference to Fig. 6, and based on (8) and (9), $f_{\text{azi}}(U_{\text{inc}}) = aU_{\text{inc}} = V_{\text{rop}}K_{\text{dls}}U_{\text{inc}}$ and $f_{\text{azi}}(U_{\text{azi}}, \beta) = aU_{\text{azi}}/\cos\beta(t)$ (recall, $\beta(t) = \pi/2 - \theta_{\text{inc}}(t))$, and $K_{\text{b}}(\widetilde{U}_{\text{azi}}, \beta)$ is given in (21).
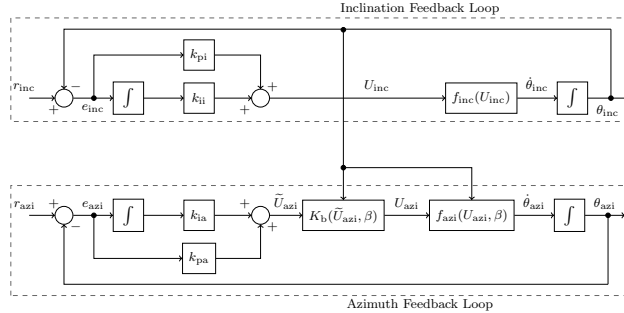

Figure 6: BPI control system

With the introduction of an augmented state, e_{ai}, representing the accumulated inclination error, and based on Fig. 7, the inclination feedback loop with

14

the PI controller is written as:

$$\dot{e}_{\mathrm{ai}}(t) = -\theta_{\mathrm{inc}}(t) \tag{22}$$

$$\dot{\theta}_{\mathrm{inc}}(t) = (k_{\mathrm{ii}}e_{\mathrm{ai}}(t) - k_{\mathrm{pi}}\theta_{\mathrm{inc}}(t))a$$

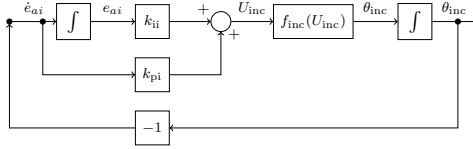where $e_{\mathrm{ai}}(t)$, $\theta_{\mathrm{inc}}(t) \in \mathbb{R}^n$ and $t \in \mathbb{R}^+$.

Figure 7: Inclination feedback loop with PI controller

Note that (22) is an LTI system and it can be put in the form of:

$$\dot{x}(t) = Ax(t), \quad t \geq 0 \tag{23}$$

$$x(0) = x_0$$

where $x \in \mathbb{R}^n$ denotes the system state, $A \in \mathbb{R}^{n \times n}$ denotes system matrix, with $x(t) = [e_{\mathrm{ai}}(t), \theta_{\mathrm{inc}}(t)]^T$ and

$$A = \begin{bmatrix} 0 & -1 \\ k_{\mathrm{ii}}a & -k_{\mathrm{pi}}a \end{bmatrix} \tag{24}$$

Clearly, the eigenvalues of A are left-half-plane for all positive a, k_{ii} and k_{pi}; hence the inclination feedback loop with the PI controller given in (24) is exponentially stable.

The remaining part of this section focuses on the stability analysis of the proposed BPI controller which is incorporated in the azimuth feedback loop (see Fig. 8). With the introduction of an augmented state, e_{aa}, representing the accumulated azimuth error, and based on Fig. 8, the azimuth feedback loop with the proposed BPI controller is written as:

$$\dot{e}_{\mathrm{aa}}(t) = -\theta_{\mathrm{azi}}(t) \tag{25}$$

$$\dot{\theta}_{\mathrm{azi}}(t) = (k_{\mathrm{ia}}e_{\mathrm{aa}}(t) - k_{\mathrm{pa}}\theta_{\mathrm{azi}}(t))af(\beta(t))$$

15

where $e_{\rm a}(t)$, $\theta_{\rm azi}(t) \in \mathbb{R}^n$; $t \in \mathbb{R}^+$,

$$f(\beta(t)) = \frac{1}{\cos\beta(t)(1 + \frac{1}{2}\beta^2(t) + \frac{5}{24}\beta^4(t))} \tag{26}$$

$\beta(t) \in [\underline{\beta}, \bar{\beta}]$ rad, $\underline{\beta}$ and $\bar{\beta}$ are the minimum and maximum values of $\beta(t)$, respectively.
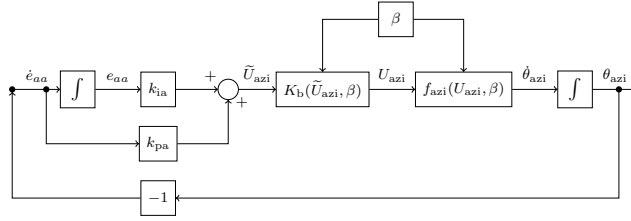

Figure 8: Azimuth feedback loop with BPI controller

Note that (25) is an LPV system and it is rewritten in a generic LPV system form (Briat, 2015, p. 10):

$$\dot{x}(t) = A(\rho(t))x(t), \quad t \geq 0 \tag{27}$$
$$x(0) = x_0$$

with: $x(t) = [e_{\rm aa}(t), \theta_{\rm azi}(t)]^T$, $\rho(t) = \beta(t)$, $A(\rho(t)) = A(\beta(t))$ and

$$A(\beta(t)) = \begin{bmatrix} 0 & -1 \\ a_1 f(\beta(t)) & -a_2 f(\beta(t)) \end{bmatrix} \tag{28}$$

where $\rho : \mathbb{R}_{\geq 0} \to \Delta_\rho$, Δ_ρ denotes the set of values of ρ, $a_1 = k_{\rm ia}a$ and $a_2 = k_{\rm pa}a$.

Furthermore, (28) is rewritten in a polytopic LPV system form (Briat, 2015, p. 56):

$$\dot{x}(t) = A(\lambda(t))x(t), \quad t \geq 0 \tag{29}$$
$$x(0) = x_0$$

16

with:

$$A(\beta(t)) = \lambda_1(t)A_1 + \lambda_2(t)A_2 \tag{30}$$

$$\lambda_1(t) = \frac{p(t) - \underline{p}}{\bar{p} - \underline{p}}, \ \lambda_2(t) = \frac{\bar{p} - p(t)}{\bar{p} - \underline{p}}, \ A_1 = \begin{bmatrix} 0 & -1 \\ a_1\underline{p} & -a_2\underline{p} \end{bmatrix}, \ A_2 = \begin{bmatrix} 0 & -1 \\ a_1\bar{p} & -a_2\bar{p} \end{bmatrix}$$

$$\tag{31}$$

where $p(t) = f(\beta(t))$, $p(t) \in [\underline{p}, \bar{p}]$, $\underline{p}$ and $\bar{p}$ are the minimum and maximum values of $p(t)$, respectively, $A(\lambda(t)) = \sum_{i=1}^{M} \lambda_i(t)A_i$, $A_i \in \mathbb{R}^{n \times n}$, $\lambda(t) \in \Lambda_M$, $\Lambda_M = \mathbf{co}\{\mathbf{V}\}$, $\mathbf{V}$ denotes a set of vertices, v_i, that is, $\mathbf{V} := \{v_1, \dots, v_M\}$, $\mathbf{V} = \mathbf{vert}\{\Lambda_M\}$ and Λ_M denotes a M-unit simplex which is defined as: $\Lambda_M := \left\{\lambda \in \mathbb{R}_{\geq 0}^n : \sum_{i=1}^{M} \lambda_i = 1\right\}$.

Based on the fact that (28) is affinely dependent on $p(t)$, (28) is rewritten in an affine parameter-dependent system form (Briat, 2015, p. 10); (Gu et al., 2013, p. 223); (Gahinet et al., 1994, 1996):

$$\dot{x}(t) = (A_{f0} + \rho_1(t)A_{f1} + \rho_2(t)A_{f2} + \cdots + \rho_n(t)A_{fn})x(t), \quad t \geq 0 \tag{32}$$
$$x(0) = x_0$$

as:

$$\dot{x}(t) = (A_{f0} + p(t)A_{f1})x(t) \tag{33}$$

where

$$A_{f0} = \begin{bmatrix} 0 & -1 \\ 0 & 0 \end{bmatrix}, \quad A_{f1} = \begin{bmatrix} 0 & 0 \\ a_1 & -a_2 \end{bmatrix} \tag{34}$$

$A_{f0}, A_{f1}, A_{f2}, \dots, A_{fn}$ are known fixed matrices and $\rho_1(t), \rho_2(t), \dots, \rho_n(t)$ are time-varying parameters.

Note that in (26) when $\beta(t) = \pi/2$ rad, $f(\beta(t)) = \infty$ which clearly leads to instability. To analyse the stability of the proposed BPI controller, $\beta(t)$ is considered as a slowly time-varying parameter with $\beta(t) \in [0, \pi/2)$ rad. Therefore, in this section, the stability of the azimuth feedback loop with the proposed BPI controller is analysed to determine the maximum value of $\bar{\beta}$, $\bar{\beta}_{max}$ such

17

240 that the azimuth feedback loop with the proposed BPI controller is stable for all $\beta(t) \in [0, \bar{\beta}_{max}]$ rad.

For the resulting Linear Matrix Inequality (LMI) problems that are described in this section, a bisection search is used to determine $\bar{\beta}_{max}$ to an arbitrary accuracy.

245 *4.1. Quadratic Stability Analysis*

4.1.1. Quadratic Stability Analysis Based on Generic LPV System

A sufficient and necessary condition for the quadratic stability of generic LPV systems is given as follows:

Theorem 1. *(Briat, 2015, p. 51); (Amato, 2006, p. 31). The generic LPV system (27) is quadratically stable if and only if there exist a matrix $\boldsymbol{P} = \boldsymbol{P}^T \succ 0$ such that the LMI*

$$A(\rho)^T \mathbf{P} + \mathbf{P} A(\rho) \prec 0 \tag{35}$$

holds for all $\rho \in \Delta_\rho$.

250 Theorem 1 does not take into consideration the rate of variation of the parameters, hence, arbitrarily fast variations of the parameters are allowed. This clearly leads to conservative stability conditions when considering systems with slowly time-varying parameters.

Theorem 1 is used to analyse the quadratic stability of the azimuth feedback loop with the proposed BPI controller given in (28), and the matrix, $\mathbf{P_g}$ is defined as:

$$\mathbf{P_g} = \begin{bmatrix} P_{g1} & P_{g2} \\ P_{g2} & P_{g3} \end{bmatrix} \succ 0 \tag{36}$$

Then, the LMI (35) becomes $A(\beta(t))^T \mathbf{P_g} + \mathbf{P_g} A(\beta(t)) \prec 0$ and it is further rewritten as:

$$\begin{bmatrix} 2P_{g2}a_1 f(\beta(t)) & P_{g1} - P_{g2}a_2 f(\beta(t)) + P_{g3}a_1 f(\beta(t)) \\ \star & -2P_{g2} - 2P_{g3}a_2 f(\beta(t)) \end{bmatrix} \prec 0 \tag{37}$$

LMI (37) is an LMI feasibility problem. With $a = V_{\mathrm{rop}} K_{\mathrm{dls}} = 4.6533 \times 10^{-3}$ rad/min, $k_{\mathrm{ia}} = 0.01$, $k_{\mathrm{pa}} = 0.13$ and $\beta(t) \in [0, \bar{\beta}_{max}]$ rad (with 0.01 increment

18

from 0 rad to $\bar{\beta}_{max}$ rad), and using a bisection search and the MATLAB LMI Toolbox, $\bar{\beta}_{max} = 1.14$ rad is obtained and an admissible solution of the matrix, $\mathbf{P_g}$ is obtained as:

$$\mathbf{P_g} = \begin{bmatrix} 1.8681 \times 10^{-6} & -1.2247 \times 10^{-5} \\ -1.2247 \times 10^{-5} & 3.6967 \times 10^{-2} \end{bmatrix} \tag{38}$$

Based on (38), LMIs (36) and (37) satisfy Theorem 1 for all $\beta(t) \in [0, 1.14]$ rad. Therefore, the azimuth feedback loop with the proposed BPI controller given in (28) is quadratically stable for all $\beta(t) \in [0, 1.14]$ rad.

4.1.2. Quadratic Stability Analysis Based on Polytopic LPV System

A sufficient and necessary condition for the quadratic stability of polytopic LPV systems is given as follows:

Theorem 2. *(Briat, 2015, p. 56). The polytopic LPV system (29) is quadratically stable if and only if there exist a matrix $\boldsymbol{P} = \boldsymbol{P}^T \succ 0$ such that the LMIs*

$$A_i^T \mathbf{P} + \mathbf{P} A_i \prec 0 \tag{39}$$

hold for all $i = 1, \ldots, M$.

Similar to Theorem 1, Theorem 2 does not take into consideration the rate of variation of the parameters, hence, arbitrarily fast variations of the parameters are allowed. This clearly leads to conservative stability conditions when considering systems with slowly time-varying parameters.

Theorem 2 is used to analyse the quadratic stability of the azimuth feedback loop with the proposed BPI controller given in (30) and (31), and the matrix, $\mathbf{P_p}$ is defined as:

$$\mathbf{P_p} = \begin{bmatrix} P_{p1} & P_{p2} \\ P_{p2} & P_{p3} \end{bmatrix} \succ 0 \tag{40}$$

Then, LMIs (39) become: $A_1^T \mathbf{P_p} + \mathbf{P_p} A_1 \prec 0$ and $A_2^T \mathbf{P_p} + \mathbf{P_p} A_2 \prec 0$, and they are further rewritten as:

$$\begin{bmatrix} -2P_{p2}a_1\underline{p} & P_{p1} - P_{p2}a_2\underline{p} + P_{p3}a_1\underline{p} \\ \star & -2P_{p2} - 2P_{p3}a_2\underline{p} \end{bmatrix} \prec 0 \tag{41}$$

19

$$
\begin{bmatrix}
-2P_{p2}a_1\bar{p} & P_{p1} - P_{p2}a_2\bar{p} + P_{p3}a_1\bar{p} \\
\star & -2P_{p2} - 2P_{p3}a_2\bar{p}
\end{bmatrix} \prec 0
\tag{42}
$$

LMIs (41) and (42) are LMI feasibility problems. With $a = V_{\text{rop}}K_{\text{dls}} = 4.6533 \times 10^{-3}$ rad/min, $k_{\text{ia}} = 0.01$, $k_{\text{pa}} = 0.13$, $\beta(t) \in [0, \bar{\beta}_{max}]$ rad and $p(t) \in [1, \bar{p}]$, and using a bisection search and the MATLAB LMI Toolbox, $\bar{\beta}_{max} = 1.1464$ rad and $\bar{p} = 1.2041$ are obtained and an admissible solution of the matrix, $\mathbf{P_p}$ is obtained as:

$$
\mathbf{P_p} =
\begin{bmatrix}
17.1594 & -1.11506 \times 10^2 \\
-1.11506 \times 10^2 & 3.3751 \times 10^5
\end{bmatrix}
\tag{43}
$$

Based on (43), LMIs (40), (41) and (42) satisfy Theorem 2 for all $\beta(t) \in [0, 1.1464]$ rad. Therefore, the azimuth feedback loop with the proposed BPI controller given in (30) and (31) is quadratically stable for all $\beta(t) \in [0, 1.1464]$ rad.

4.1.3. Quadratic Stability Analysis Based on Affine Parameter-Dependent System

The quadratic stability of the affine parameter-dependent system, (32) can be analysed by the MATLAB function quadstab which takes into consideration solution of various LMI while attempting to find a positive definite quadratic Lyapunov function of the form:

$$
V(x) = x^T \mathbf{P} x
\tag{44}
$$

such that $dV(x)/dt < 0$ along all state trajectories (Gu et al., 2013, p. 229). For the quadratic Lyapunov function given in (44), the stability condition $dV(x)/dt < 0$ is equivalent to

$$
(A_{f0} + \rho_1(t)A_{f1} + \cdots + \rho_n(t)A_{fn})^T\mathbf{P} + \mathbf{P}(A_{f0} + \rho_1(t)A_{f1} + \cdots + \rho_n(t)A_{fn}) \prec 0
\tag{45}
$$

Nonetheless, owing to the fact that arbitrarily fast variations of parameters are allowed by the MATLAB function quadstab, the MATLAB function quadstab

20

provides conservative stability results when considering systems with slowly time-varying parameters.

The MATLAB function `quadstab` is used to analyse the quadratic stability of the azimuth feedback loop with the proposed BPI controller given in (33), and the matrix $\mathbf{P_a}$ is defined as:

$$\mathbf{P_a} = \begin{bmatrix} P_{a1} & P_{a2} \\ P_{a2} & P_{a3} \end{bmatrix} \succ 0 \tag{46}$$

Then, the LMI (45) becomes:

$$(A_{f0} + p(t)A_{f1})^T \mathbf{P_a} + \mathbf{P_a}(A_{f0} + p(t)A_{f1}) \prec 0 \tag{47}$$

and it is further rewritten as:

$$\begin{bmatrix} -2P_{a2}a_1 p(t) & P_{a1} - P_{a2}a_2 p(t) + P_{a3}a_1 p(t)) \\ \star & -2P_{a2} - 2P_{a3}a_2 p(t) \end{bmatrix} \prec 0 \tag{48}$$

LMI (48) is an LMI feasibility problem. With $a = V_{\mathrm{rop}}K_{\mathrm{dls}} = 4.6533 \times 10^{-3}$ rad/min, $k_{\mathrm{ia}} = 0.01$, $k_{\mathrm{pa}} = 0.13$ and $\beta(t) \in [0, \bar{\beta}_{max}]$ rad, and using a bisection search and the MATLAB function `quadstab`, $\bar{\beta}_{max} = 1.1464$ rad is obtained and an admissible solution of the matrix, $\mathbf{P_a}$ is obtained as:

$$\mathbf{P_a} = \begin{bmatrix} 3.9125 \times 10^{-6} & -2.5457 \times 10^{-5} \\ -2.5457 \times 10^{-5} & 7.6956 \times 10^{-2} \end{bmatrix} \tag{49}$$

Based on (49), LMIs (46) and (48) satisfy LMI (45) for all $\beta(t) \in [0, 1.1464]$ rad. Therefore, the azimuth feedback loop with the proposed BPI controller given in (33) is quadratically stable for all $\beta(t) \in [0, 1.1464]$ rad.

Comparing the quadratic stability results obtained from Theorems 1 and 2 and the MATLAB function `quadstab`, $\bar{\beta}_{max} = 1.14$ rad is obtained from Theorem 1 and $\bar{\beta}_{max} = 1.1464$ rad is obtained from Theorem 2 and the MATLAB function `quadstab` (also see Table 2). Hence, a more conservative stability result is obtained from Theorem 1 than that obtained from Theorem 2 and the MATLAB function `quadstab`.

The stability notions for the generic LPV, polytopic LPV and affine parameter-dependent systems to be quadratically stable considered in this subsection does

21

not take into consideration the rate of variation of the parameters, hence, arbitrarily fast variations of the parameters are allowed. As expected, this clearly leads to conservative stability conditions while considering systems with slowly time-varying parameters, such as (25). To reduce the conservatism of the quadratic stability, the subsequent subsection presents the analysis of robust stability which takes into consideration the rate of variation of the parameters.

4.2. Robust Stability Analysis

4.2.1. Robust Stability Analysis Based on Affine Parameter-Dependent System

The robust stability of the affine parameter-dependent system, (32) can be analysed by the MATLAB function `pdlstab` which takes into consideration solution of various LMIs while attempting to find a positive definite parameter-dependent Lyapunov function of the form:

$$V(x, \rho) = x^T Q(\rho)^{-1} x \tag{50}$$

where $Q(\rho) = Q_0 + \rho_1 Q_1 + \rho_2 Q_2 + \cdots + \rho_n Q_n$ and $Q_0, Q_1, Q_2, \ldots, Q_n$ are symmetric matrices, such that $dV(x, \rho)/dt < 0$ along all admissible trajectories (Gu et al., 2013, p. 229). For the parameter-dependent Lyapunov function given in (50), the stability condition $dV(x, \rho)/dt < 0$ is equivalent to

$$
\begin{aligned}
Q(\rho)(A_{f0} + \rho_1(t)A_{f1} + \cdots + \rho_n(t)A_{fn})^T \\
+ (A_{f0} + \rho_1(t)A_{f1} + \cdots + \rho_n(t)A_{fn})Q(\rho) - \frac{dQ(\rho)}{dt} \prec 0
\end{aligned}
\tag{51}
$$

In the case of systems with slowly varying or constant parameters, less conservative stability results could be obtained by the MATLAB function `pdlstab` (Gu et al., 2013, p. 229).

The MATLAB function `pdlstab` is used to analyse the robust stability of the azimuth feedback loop with the proposed BPI controller given in (33), and the matrix $Q(p(t))$ is defined as:

$$Q(p(t)) = Q_0 + p(t)Q_1 \succ 0 \tag{52}$$

Then, the LMI (51) becomes:

$$Q(p(t))(A_{f0} + p(t)A_{f1})^T + (A_{f0} + p(t)A_{f1})Q(p(t)) - \frac{dQ(p(t))}{dt} \prec 0 \qquad (53)$$

LMI (53) is an LMI feasibility problem. With $a = V_{\text{rop}}K_{\text{dls}} = 4.6533 \times 10^{-3}$ rad/min, $k_{\text{ia}} = 0.01$, $k_{\text{pa}} = 0.13$ and $\beta(t) \in [0, \bar{\beta}_{max}]$ rad, and using a bisection search and the MATLAB function `pdlstab`, $\bar{\beta}_{max} = 1.1464$ rad is obtained and an admissible solution of the matrices, Q_0 and Q_1 are obtained as:

$$Q_0 = \begin{bmatrix} 9.5986 \times 10^6 & 3.1746 \times 10^3 \\ 3.1746 \times 10^3 & 4.88 \times 10^2 \end{bmatrix}, \quad Q_1 = \begin{bmatrix} -7.1775 & 0.0929 \\ 0.0929 & 0.0019 \end{bmatrix} \qquad (54)$$

Based on (54), LMIs (52) and (53) are satisfied for all $\beta(t) \in [0, 1.1464]$. Therefore, the azimuth feedback loop with the proposed BPI controller given in (33) is robustly stable for all $\beta(t) \in [0, 1.1464]$ rad.

4.2.2. Robust Stability Analysis Based on Polytopic LPV System

The rate of variation of the parameters is captured in the term $\dot{\lambda}$. To define a set that contains the trajectories of $\dot{\lambda}$, it is assumed that the polytopic LPV system, (29) approximates the generic LPV system, (27) with M_p parameters, given by ρ, where the bounds of the derivative are known (Briat, 2015, p. 57). Hence, a polytope where $\dot{\lambda}$ evolves within is defined from the following proposition:

Proposition 1. *(Briat, 2015, p. 58). Assume that $\dot{\rho} \in \Delta_\nu = \boldsymbol{co}\{\boldsymbol{V}_\nu\}, \boldsymbol{V}_\nu = \{d_1, \ldots, d_M\}, M = 2^{M_p}$ and that the decomposition*

$$\rho(t) = \sum_{i=1}^{M} \lambda_i(t)v_i \qquad (55)$$

holds with $\boldsymbol{V}_\rho = \{v_1, \ldots, v_M\}$. Then, the set of all $\dot{\lambda}$'s is given by

$$\dot{\Lambda}_M := \left\{ \begin{bmatrix} \mathbf{V} \\ \mathbf{1}_M^T \\ \mathbf{0}_M \end{bmatrix}^+ \begin{bmatrix} \mathbf{D} \\ \mathbf{0}_M \\ \mathbf{1}_M^T \end{bmatrix} \zeta : \zeta \in \Lambda_M \right\} \qquad (56)$$

23

where $\mathbf{1}_M$ denotes a column vector of dimension M containing 1 entries, $\mathbf{0}_M$
denotes a row vector of dimension M containing 0 entries, $\mathbf{D}$ denotes a set of
vertices, d_i, that is, $\mathbf{D} = [d_1, \ldots, d_M]$, $\mathbf{V} = [v_1, \ldots, v_M]$ and $\zeta(t) \in \Lambda_M$. In
addition, the following identity is obtained:

$$\dot{\rho}(t) = \sum_{i=1}^{M} \dot{\lambda}_i(t)v_i = \sum_{i=1}^{M} \zeta_i(t)d_i \tag{57}$$

From Proposition 1, a matrix of vertex points, $\mathbf{vert}\{\dot{\Lambda}_M\}$ can be defined as:

$$\mathbf{L} = \begin{bmatrix} \mathbf{V} \\ \mathbf{1}_M^T \\ \mathbf{0}_M \end{bmatrix}^{+} \begin{bmatrix} \mathbf{D} \\ \mathbf{0}_M \\ \mathbf{1}_M^T \end{bmatrix} \tag{58}$$

The robust stability of the polytopic system, (29) can be analysed by the
following theorem:

Theorem 3. *(Briat, 2015, p. 61). The polytopic LPV system (29) is robustly*
stable if there exist matrices $\boldsymbol{P}_i = \boldsymbol{P}_i^T \succ 0, i = 1, \ldots, M$, a matrix $\boldsymbol{X} \in \mathbb{R}^{n \times n}$
and a sufficiently large scalar $\xi > 0$ such that the matrix inequalities

$$\begin{bmatrix} -(\mathbf{X} + \mathbf{X}^T) & \mathbf{P}_i + \mathbf{X}^T A_i & \mathbf{X}^T \\ \star & -\xi\mathbf{P}_i + \sum_{j=1}^{M} \mathbf{P}_j l_{ji} & 0 \\ \star & \star & -\mathbf{P}_i/\xi \end{bmatrix} \prec 0 \tag{59}$$

hold for all $i = 1, \ldots, M$, where l_{ji} are the elements of $\mathbf{L}$.

Theorem 3 takes into consideration the rate of variation of the parameters,
hence, provides less conservative stability results.

Theorem 3 is used to analyse the robust stability of the polytopic LPV
system given in (30) and (31). Based on Theorem 3, the rate of variation of
the parameters is captured in the term $\dot{\lambda}$. To define a set that contains the
trajectories of $\dot{\lambda}$, it is assumed that the polytopic LPV system, (30) and (31)
approximates the generic LPV system, (28) with M_p parameters, given by ρ,
where the bounds of the derivative are known. Hence, a polytope where $\dot{\lambda}$
evolves within is defined from Proposition 1.

In this case, and with reference to Proposition 1 and (58), $\mathbf{V} = p(t) = [\underline{p}, \bar{p}]$, $\mathbf{D} = \dot{p}(t) = [\underline{\dot{p}}, \bar{\dot{p}}]$, $\bar{\dot{p}} = (\overline{dp/d\beta})\bar{\dot{\beta}}$ and $\underline{\dot{p}} = -(\overline{dp/d\beta})\bar{\dot{\beta}}$; where $\overline{dp/d\beta}$ is the maximum value of $dp/d\beta$ and $\bar{\dot{\beta}}$ is the maximum value of $\dot{\beta}$ and it is considered as the maximum possible build rate, that is, $\bar{\dot{\beta}} = V_{\mathrm{rop}}K_{\mathrm{dls}}$. Furthermore, for a time-varying single parameter system such as (30) and (31), $M_p = 1$ and $M = 2^{M_p} = 2$, the resulting form of (58) evaluation is:

$$\mathbf{L} = \begin{bmatrix} l_{11} & l_{12} \\ l_{21} & l_{22} \end{bmatrix} \tag{60}$$

where l_{11}, l_{12}, l_{21} and l_{22} are the elements of $\mathbf{L}$.

Based on Theorem 3 and the azimuth feedback loop with the proposed BPI controller given in (30) and (31), and given the matrices, $\mathbf{P_1}$, $\mathbf{P_2}$ and $\mathbf{X}$, the LMIs (59) become:

$$\begin{bmatrix} -(\mathbf{X} + \mathbf{X}^T) & \mathbf{P_1} + \mathbf{X}^T A_1 & \mathbf{X}^T \\ \star & -\xi\mathbf{P_1} + \mathbf{P_1}l_{11} + \mathbf{P_2}l_{21} & 0 \\ \star & \star & -\mathbf{P_1}/\xi \end{bmatrix} \prec 0 \tag{61}$$

$$\begin{bmatrix} -(\mathbf{X} + \mathbf{X}^T) & \mathbf{P_2} + \mathbf{X}^T A_2 & \mathbf{X}^T \\ \star & -\xi\mathbf{P_2} + \mathbf{P_1}l_{12} + \mathbf{P_2}l_{22} & 0 \\ \star & \star & -\mathbf{P_2}/\xi \end{bmatrix} \prec 0 \tag{62}$$

LMIs (61) - (62) are LMI feasibility problems. With $a = \bar{\dot{\beta}} = V_{\mathrm{rop}}K_{\mathrm{dls}} = 4.6533 \times 10^{-3}$ rad/min, $k_{\mathrm{ia}} = 0.01$, $k_{\mathrm{pa}} = 0.13$, $\beta(t) \in [0, \bar{\beta}_{max}]$ rad and $p(t) \in [1, \bar{p}]$, and using a *line-search algorithm*[1], a bisection search and the MATLAB LMI Toolbox, the following are obtained: $\xi = 0.9$, $\bar{\beta}_{max} = 1.5707$ rad, $\bar{p} = 2964.8$, $\underline{\dot{p}} = -143200$, $\bar{\dot{p}} = 143200$, $l_{11} = l_{22} = 48.3171$ and $l_{12} = l_{21} = -48.3171$.

---

[1]A line-search algorithm continuously increases the value of ξ until the problem becomes feasible, or terminates when the value of ξ exceeds a particular limit value.

Also, admissible solutions of the matrices, $\mathbf{P_1}$, $\mathbf{P_2}$ and $\mathbf{X}$ are obtained as follows:

$$\mathbf{P_1} = \begin{bmatrix} 86.2156 & -60.6632 \\ -60.6632 & 317.9908 \end{bmatrix}, \quad \mathbf{P_2} = \begin{bmatrix} 86.4084 & -62.1581 \\ -62.1581 & 322.5416 \end{bmatrix}, \quad (63)$$

$$\mathbf{X} = \begin{bmatrix} 89.7116 & 11.7048 \\ -92.0640 & 175.3409 \end{bmatrix} \quad (64)$$

The matrices, $\mathbf{P_1}$, $\mathbf{P_2}$ and $\mathbf{X}$ given in (63) and (64), and $\xi = 0.9$ satisfy Theorem 3 for all $\beta(t) \in [0, 1.5707]$ rad. Therefore, the azimuth feedback loop with the proposed BPI controller given in (30) and (31) is robustly stable for all $\beta(t) \in [0, 1.5707]$ rad.

Comparing the robust stability results obtained from the MATLAB function `pdlstab` and Theorem 3, $\bar{\beta}_{max} = 1.1464$ rad is obtained from the MATLAB function `pdlstab` and $\bar{\beta}_{max} = 1.5707$ rad is obtained from Theorem 3. Unexpectedly, for this particular case, the MATLAB function `pdlstab` gives a conservative stability result as against an expected less conservative stability result and it is the same result as those obtained from Theorem 2 and the MATLAB function `quadstab` (in Subsection 4.1) as shown in Table 2. Expectedly, Theorem 3 gives a less conservative stability result as the stability result proves that the azimuth feedback loop with the proposed BPI controller is robustly stable for nearly the whole range of operations, $\beta(t) \in [0, \pi/2]$ rad, within practical engineering accuracy.

Table 2: $\bar{\beta}_{max}$ for Different LPV Stability Notions

LPV Stability Notion	$\bar{\beta}_{max}$
Theorem 2.2	1.1400 rad
Theorem 2.3	1.1464 rad
MATLAB function `quadstab`	1.1464 rad
MATLAB function `pdlstab`	1.1464 rad
Theorem 2.4	1.5707 rad

Based on the fact that the inclination feedback loop with the PI controller is shown to be exponentially stable and the azimuth feedback loop with the pro-

posed BPI controller is proven to be quadratically and robustly stable, therefore, the proposed BPI control system is proven to be stable.

5. Simulation Results

In this section, the transient simulations are carried out using MATLAB/Simulink. The system delays are implemented as $e^{-\tau_d s}$, where τ_d is the time delay. The τ_d is dependent on the V_{rop} and the distance of the D&I sensor from the bit, d_t which is given by

$$\tau_d = \frac{d_t}{V_{\mathrm{rop}}} \tag{65}$$

5.1. Low-Fidelity Model Simulation

Using the nonlinear system given by (2) and (3), the proposed BPI controller and the systems delays, MATLAB/Simulink transient simulations are created based on the LFM scheme, shown in Fig. 9, to analyse the effectiveness, robustness and stability of the proposed BPI controller over the PI controller proposed by Panchal et al. (2010). The parameters used for the LFM simulations are given in Table 3. In the interest of viewing the dynamic responses, the saturation effect is removed. A reference change of 0.015 rad for a set of various azimuth angles of $\pi/18$ rad, $\pi/9$ rad, $\pi/6$ rad, $\pi/3$ rad and $\pi/2$ rad are implemented to investigate the invariance of the azimuth responses of the proposed BPI controller and the PI controller proposed by Panchal et al. (2010).
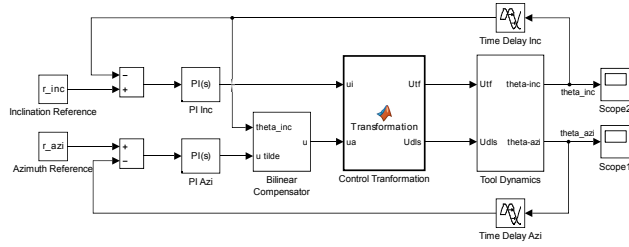

Figure 9: Simulink diagram of LFM simulation scheme for BPI controller

Based on the LFM simulation, the PI controller proposed by Panchal et al. (2010) and the proposed BPI controller azimuth responses for a reference change

27

Table 3: Simulation Parameters for BPI Controller with LFM

Parameter	Value	Parameter	Value
θ_{inc}	$\pi/6$ rad (30°)	k_{ii}	0.01
θ_{azi}	$\pi/6$ rad (30°)	k_{pa}	0.13
V_{rop}	200 ft/hr (1.0158 m/min)	k_{ia}	0.01
K_{dls}	8°/100 ft (4.5809e-3 rad/m)	k_{pi}	0.15
V_{dr}	1°/100 ft (5.7261e-4 rad/m)	r_{inc}	$\pi/6 + 0.015$ rad
V_{tr}	0.5°/100 ft (2.8631e-4 rad/m)	r_{azi}	$\pi/6 + 0.015$ rad
d_t	14.997 ft (4.5711 m)	τ_d	4.5 min

of 0.015 rad for a set of various azimuth angles are shown in Figs. 10 and 11, respectively, where $\Delta\theta_{\mathrm{azi}}(t) = \theta_{\mathrm{azi}}(t) - \theta_{\mathrm{azi}}(0)$ and $\tau_d = 0$ min. Comparing the

355 azimuth responses of the PI controller proposed by Panchal et al. (2010) and the proposed BPI controller, the proposed BPI controller azimuth responses tend to converge more closely to the nominal operating point of $\pi/2$ rad, than the PI controller proposed by Panchal et al. (2010) azimuth responses. Hence, the proposed BPI controller provides more consistent azimuth responses over wider

360 range of the directional drilling tool operations, than the PI controller proposed by Panchal et al. (2010).
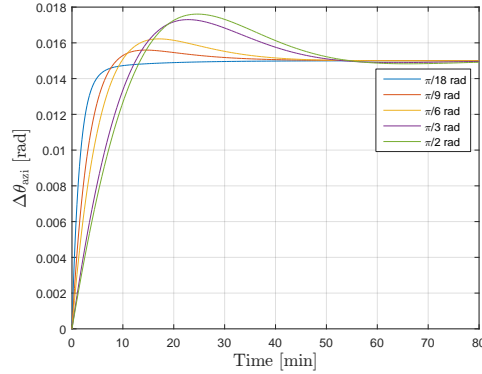

Figure 10: PI controller (proposed by Panchal et al. (2010)) azimuth response with LFM
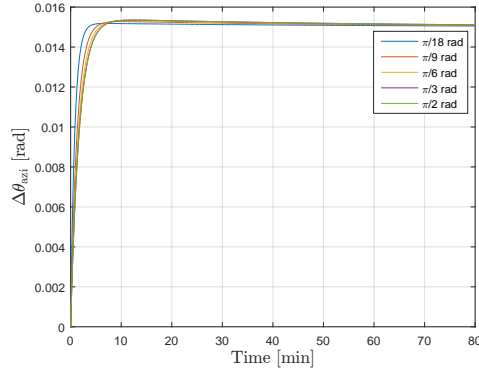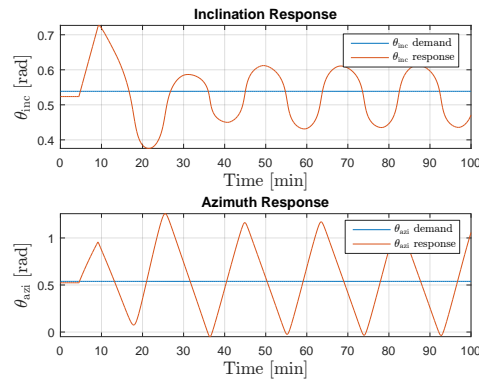
Figure 11: BPI controller azimuth response with LFM

Figure 12: PI controller (proposed by Panchal et al. (2010)) attitude response with LFM

To investigate the adverse effects of disturbances and time delay on the feedback measurements with respect to the stability and performance of the directional drilling tool, the inclination and azimuth responses to step changes of the PI controller proposed by Panchal et al. (2010) and the proposed BPI controller based on the LFM simulation are shown in Figs. 12 and 13, respectively.

The inclination and azimuth responses to step changes, from $\pi/6$ rad to $\pi/6 + 0.015$ rad and from $\pi/6$ to $\pi/6 + 0.015$ rad, respectively, of the PI controller proposed by Panchal et al. (2010) are shown in Fig. 12. The attitude response of the PI controller proposed by Panchal et al. (2010) exhibits oscillatory characteristics. Hence, the inclination and azimuth responses of the
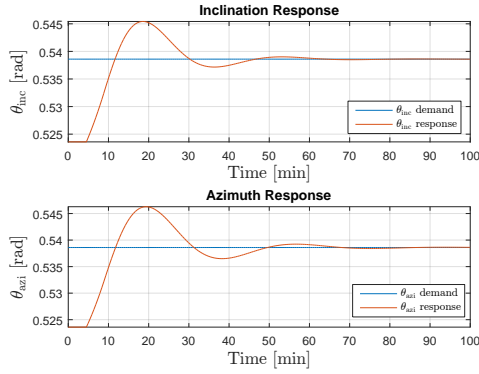
29

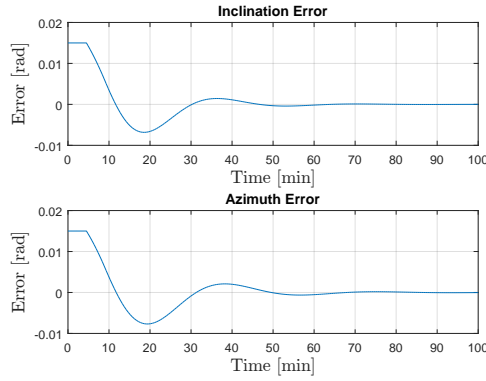Figure 13: BPI controller attitude response with LFM

Figure 14: Attitude error for BPI controller with LFM

directional drilling tool do not converge to the desired angles of $\pi/6 + 0.015$ rad and $\pi/6 + 0.015$ rad, respectively, as the PI controller proposed by Panchal et al. (2010) is unable to handle the adverse effects of the drop rate disturbance of up to $1°/100$ ft, turn rate bias disturbance of up to $0.5°/100$ ft and time delay of up to 4.5 min on the feedback measurements.

The inclination and azimuth responses to step changes, from $\pi/6$ rad to $\pi/6 + 0.015$ rad and from $\pi/6$ rad to $\pi/6 + 0.015$ rad, respectively, of the proposed BPI controller are shown in Fig. 13. The inclination and azimuth responses of the directional drilling tool converges to the desired angles of $\pi/6 + 0.015$ rad and $\pi/6 + 0.015$ rad, respectively. Hence, the proposed BPI controller reduces

30

the adverse effects of the drop rate disturbance of up to $1°/100$ ft, turn rate bias disturbance of up to $0.5°/100$ ft and time delay of up to 4.5 min on the feedback measurements with respect to the stability and performance, than the PI controller proposed by Panchal et al. (2010).

The inclination and azimuth errors for the proposed BPI controller are shown in Fig. 14. The proposed BPI controller is able to converge the inclination and azimuth errors directly to zero within 62 min.

5.2. High-Fidelity Model Simulation

Using the nonlinear system given by (2) and (3), the proposed BPI controller, the systems delays and the drilling cycle scheme presented in Inyang (2017), MATLAB/Simulink transient simulations are created based on the HFM simulation scheme, shown in Fig. 15, to further analyse the effectiveness, robustness and stability of the proposed BPI controller. The parameters used for the HFM simulations are given in Table 4. The values of τ_d, k_{ia}, k_{pa}, k_{ii}, k_{pi}, V_{dr}, V_{tr} and d_t are the same as those for the LFM simulation (see Table 3).

Table 4: Simulation Parameters for BPI Controller with HFM

Parameter	Value	Parameter	Value
V_{rop}	200 ft/hr (1.0158 m/min)	θ_{inc}	$\pi/2$ rad (90°)
K_{dls}	$8°/100$ ft (4.5809e-3 rad/m)	θ_{azi}	$\pi/2$ rad (90°)
T_a	0.05 s (8.333e-4 min)	r_{inc}	$\pi/2 + 0.015$ rad
k_{vi}	6 s^{-1} (360 min^{-1})	r_{azi}	$\pi/2 + 0.015$ rad
$\hat{\omega}_{tf}$	2π rad/s (376.991 rad/min)	k_p	1 s^{-1} (60 min^{-1})
t_{cycle}	10 s (0.1667 min)	k_{vp}	0.5

Based on the HFM simulation, the inclination and azimuth responses to step changes, from $\pi/2$ rad to $\pi/2 + 0.015$ rad and from $\pi/2$ rad to $\pi/2 + 0.015$ rad, respectively, of the proposed BPI controller are shown in Fig. 16. The proposed BPI controller still holds the inclination and azimuth of the directional drilling
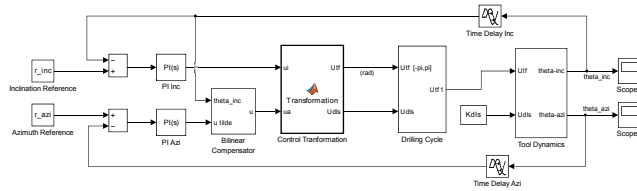
31

Figure 15: Simulink diagram of HFM simulation scheme for BPI controller
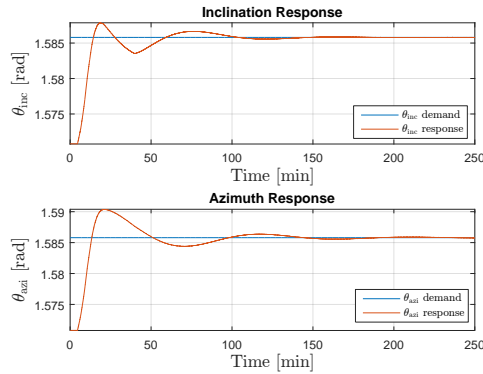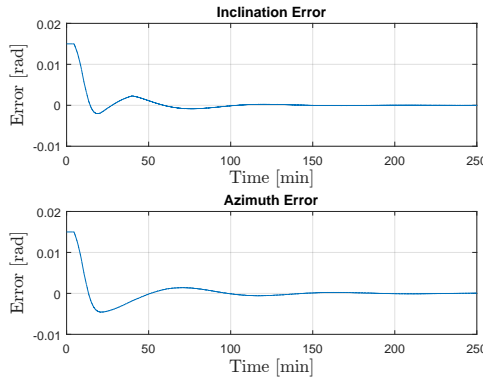

Figure 16: BPI controller attitude response with HFM

Figure 17: Attitude error for BPI controller with HFM

tool at the desired angles of $\pi/2 + 0.015$ rad and $\pi/2 + 0.015$ rad, respectively. Hence, the proposed BPI controller is effective, stable and robust to handle the adverse effects of the drop rate disturbance of up to $1°/100$ ft, turn rate bias disturbance of up to $0.5°/100$ ft, time delay of up to 4.5 min on the feedback measurements and some other uncertainties (such as drilling cycle and toolface

32

actuator dynamics) in the attitude control of the directional drilling tool.

The inclination and azimuth errors for the proposed BPI controller with the HFM are shown in Fig. 17. The proposed BPI controller is able to converge the inclination and azimuth errors directly to zero within 150 min.

6. Conclusions

This paper proposes a bilinear model of directional drilling tool. The proposed bilinear model characterises the nonlinear properties of directional drilling tool more accurately than the existing linear model. Hence, it broadens the range of adequate performance and it is considered to be significantly advantageous in application to directional drilling operations. The proposed bilinear model is used as the basis for the design of a Bilinear Proportional plus Integral (BPI) controller for the attitude control of directional drilling tool.

The proposed BPI control system is proven to be stable using stability notions for LTI and LPV systems. The proposed BPI controller is able hold the attitude of the directional drilling tool at the desired inclination and azimuth angles, provide more consistent azimuth responses over wider range of directional drilling operations and significantly reduces the adverse effects of time delay of up to 4.5 min on the feedback measurements, drop rate disturbance of up to $1°/100$ ft, turn rate bias disturbance of up to $0.5°/100$ ft, and some other uncertainties (such as drilling cycle and toolface actuator dynamics) in the attitude control of the directional drilling tool. However, the proposed BPI controller is restricted to attitudes such that θ_{inc} is not close to $0°$, and also, the performance of the proposed BPI controller reduces as the time delay, drop rate disturbance and turn rate bias disturbance increases above 4.5 min, $1°/100$ ft and $0.5°/100$ ft, respectively.

The proposed BPI controller is relatively simple and it can easily be implemented in the directional drilling tools to increase the potential of accessing difficult reservoirs, drilling more effectively and cost-effective field development. The implementation of the proposed BPI controller should reduce the workload

33

of the directional driller because with the significant reduction of the adverse effects of measurement delay and disturbances during directional drilling operations, the directional drilling tool will drill more effectively, hence a less intervention is required from the directional driller.

Stability proof of the proposed BPI controller with time delay remains an open problem.

References

Al-zahrani, A.A., Wali, M.M., 1994. An adaptive bilinear model-predictive control algorithm for a plate heat exchanger. Developments in Chemical Engineering and Mineral Processing 2, 158–170.

Amato, F., 2006. Robust Control of Linear Systems Subject to Uncertain Time-Varying Parameters. volume 325. Springer, Berlin.

Baker, R., 1996. A Primer of Oilwell Drilling. 5th (revised) ed., The University of Texas at Austin in cooperation with International Association of Drilling Contractors, Texas, USA.

Bayliss, M.T., Inyang, I.J., Whidborne, J.F., 2015. Application of LQG control to attitude control of directional drilling, in: 24th International Conference on Systems Engineering, Coventry, UK.

Bayliss, M.T., Whidborne, J.F., 2015. Mixed uncertainty analysis of pole placement and H_∞ controllers for directional drilling attitude tracking. Journal of Dynamic Systems, Measurement, and Control 137, 121008.

Briat, C., 2015. Linear Parameter-Varying and Time-Delay Systems: Analysis, Observation, Filtering & Control. Springer, Berlin, Heidelberg.

Bruni, C., DiPillo, G., Koch, G., 1974. Bilinear systems: An appealing class of nearly linear systems in theory and applications. IEEE Transactions on Automatic Control AC-19, 334–348.

Burnham, K.J., Dunoyer, A., Marcroft, S., 1999. Bilinear controller with PID structure. Computing and Control Engineering Journal 10, 63–69.

Chen, Y.P., Chang, J.L., Lai, K.M., 2000. Stability analysis and bang-bang sliding control of a class of single-input bilinear systems. IEEE Transactions on Automatic Control 45, 2150–2154.

Cockburn, C., Matheus, J., Dang, K.L.P., 2011. Automatic trajectory control in extended-reach wells, in: SPE Middle East Oil and Gas Show and Conference, Manama, Bahrain.

Devereux, S., 1999. Drilling Technology in Nontechnical Language. PennWell Corporation, OK.

Downton, G.C., 2012. Challenges of modeling drilling systems for the purposes of automation and control, in: IFAC Workshop on Automatic Control in Offshore Oil and Gas Production, Trondheim, Norway.

Downton, G.C., 2014. Systems modeling and design of automated-directional-drilling systems, in: SPE Annual Technical Conference and Exhibition, Amsterdam, Netherlands.

Gahinet, P., Apkarian, P., Chilali, M., 1994. Affine parameter-dependent lyapunov functions for real parameteric uncertainty, in: 33rd Conference on Decision and Control, FL.

Gahinet, P., Apkarian, P., Chilali, M., 1996. Affine parameter-dependent lyapunov functions and real parameteric uncertainty. IEEE Transactions on Automatic Control 41, 436–442.

Genevois, J., Boulet, J., Simon, C., Reullon, C., 2003. Gyrostab project: The missing link azimuth and inclination mastered with new principles for standard rotary BHAs, in: SPE/IADC Drilling Conference, Amsterdam, Netherlands.

Ghasemi, M., Ibrahim, A., Gildin, E., 2014. Reduced order modeling in reservoir simulation using the bilinear approximation techniques, in: SPE Latin American and Caribbean Petroleum Engineering Conference, Maracaibo, Venezuela.

Goodhart, S.G., Burnham, K.J., James, D.J.G., 1994. Bilinear self-tuning control of a high temperature heat treatment plant. IEEE Proceedings: Control Theory and Applications 141, 12–18.

Gu, D.W., Petkov, P.H., Konstantinov, M.M., 2013. Robust Control Design with MATLAB. 2nd ed., Springer Verlag, London.

Inyang, I.J., 2017. Attitude Control of Directional Drilling. Ph.D. thesis. Cranfield University. Cranfield, UK.

Inyang, I.J., Whidborne, J.F., Bayliss, M.T., 2016. Bilinear modelling and bilinear PI control of directional drilling, in: 11th UKACC International Conference on Control, Belfast, UK.

Jijón, R.B., Canudas-de-Wit, C., Niculescu, S.I., Dumon, J., 2010. Adaptive observer design under low data rate transmission with applications to oil well drill-string, in: American Control Conference, Baltimore, MD.

Kelman, A., Borrelli, F., 2011. Bilinear model predictive control of a HVAC system using sequential quadratic programming, in: 18th IFAC World Congress, Milan, Italy. pp. 9896–9874.

Kim, B., Lim, M., 2003. Robust H_{∞} control method for bilinear systems. International Journal of Control, Automation and Systems 1, 171–177.

Kremers, N.A.H., Detournay, E., van de Wouw, N., 2016. Model-based robust control of directional drilling systems. IEEE Transactions on Control Systems Technology 24, 226–239.

Krener, A.J., 1974. Linearization and bilinearization of control systems, in: Proc. 12th Allerton Conference on Circuits and Systems, Monticello, IL. pp. 834–843.

Kuwana, S., Kiyosawa, Y., Ikeda, A., 1994. Attitude control device and drilling-direction control device. Patent US5307885 A.

Lim, D., Rasmussen, B.P., Swaroop, D., 2009. Selecting PID control gains for nonlinear HVAC&R systems. HVAC&R Research 15, 991–1019.

Martineau, S., Burnham, K.J., Haas, O.C.L., Andrews, G., Heeley, A., 2004. Four-term bilinear PID controller applied to an industrial furnace. Control Engineering Practice 12, 457–464.

Martineau, S., Burnham, K.J., Minihan, J.A., Marcroft, S., Andrews, G., Heeley, A., 2002. Application of a bilinear PID compensator to an industrial furnace, in: 15th IFAC World Congress on Automatic Control, Barcelona, Spain.

Matheus, J., Ignova, M., Hornblower, P., 2012. A hybrid approach to closed-loop directional drilling control using rotary steerable systems, in: Proceedings of the 2012 IFAC Workshop on Automatic Control in Offshore Oil and Gas Production, Trondheim, Norway.

Matheus, J., Ignova, M., Hornblower, P., 2014. A hybrid approach to closed-loop directional drilling control using rotary steerable systems, in: SPE Latin American and Caribbean Petroleum Engineering Conference, Maracaibo, Venezuela.

Matheus, J., Naganathan, S., 2010. Drilling automation: Novel trajectory control algorithms for RSS, in: IADC/SPE Drilling Conference and Exhibition, New Orleans, LA.

Panchal, N., 2013. Autonomous Trajectory Control for Directioanal Drilling. Ph.D. thesis. Cranfield University. Cranfield, UK.

Panchal, N., Bayliss, M.T., Whidborne, J.F., 2010. Robust linear feedback control of attitude for directional drilling tools, in: 13th IFAC Symposium on Automation in Mining, Mineral and Metal Processing, Cape Town, South Africa.

Park, R.W., Lee, K.T., 2009. Design of a bilinear robust controller for a hydrostatic driver, in: IEEE International Symposium on Industrial Electronics, Seoul, Korea. pp. 1470–1475.

Pedersen, M., Lechner, M., Pon, Z., Brink, D., Abbasy, I., Jaafar, M., 2009. Case study: Successful application of a novel conformance treatment in an extended reach horizontal well in the Al Shaheen field, offshore Qatar, in: SPE Offshore Europe Oil & Gas Conference & Exhibition, Aberdeen, UK.

Qian, K., Zhang, Y., 2014. Bilinear model predictive control of plasma keyhole pipe welding process. Journal of Manufacturing Science and Engineering, Transactions of the ASME 136, 031002–1 – 031002–10.

Rade, L., Westergren, B., 1999. Mathematics Handbook for Science and Engineering. 4th ed., Springer, Berlin - Tokyo.

Rugh, W.J., 1981. Nonlinear System Theory: The Volterra/Wiener Approach. Johns Jopkins University Press, Baltimore, MD.

Schwarz, H., Dorissen, H.T., 1989. System identification of bilinear systems via realization theory and its application. Control, Theory and Advanced Technology 5, 137–155.

Short, J.A., 1993. Introduction to Directional and Horizontal Drilling. PennWell Publishing Company, OK.

van de Wouw, N., Monsieurs, F.H.A., Detournay, E., 2016. Dynamic state-feedback control of nonlinear three-dimensional directional drilling systems. IFAC-PapersOnLine 49, 85–90.

Yinghui, L., Yinao, S., 2000. Automatic inclination controller: A new inclination controlling tool for rotary drilling, in: IADC/SPE Drilling Conference, New Orleans, LA.

Yonezawa, T., Cargill, E., Gaynor, T., Hardin, J., Hay, R., Ikeda, A., Kiyosawa, Y., 2002. Robotic controlled drilling: A new rotary steerable drilling system for the oil and gas industry, in: IADC/SPE Drilling Conference, Texas, USA.